

## Characterization of radio frequency plasma using Langmuir probe and optical emission spectroscopy

M. Nisha, K. J. Saji, R. S. Ajimsha, N. V. Joshy, and M. K. Jayaraj<sup>a)</sup>  
*Optoelectronics Devices Laboratory, Department of Physics, Cochin University of Science and Technology, Kochi-682 022, Kerala, India*

(Received 21 February 2005; accepted 4 January 2006; published online 15 February 2006)

The radio frequency plasma generated during the sputtering of Indium Tin Oxide target using Argon was analyzed by Langmuir probe and optical-emission spectroscopy. The basic plasma parameters such as electron temperature and ion density were evaluated. These studies were carried out by varying the RF power from 20 to 50 W. A linear increase in ion density and an exponential decrease in electron temperature with rf power were observed. The measured plasma parameters were then correlated with the properties of ITO thin films deposited under similar plasma conditions. © 2006 American Institute of Physics. [DOI: 10.1063/1.2171777]

### I. INTRODUCTION

Magnetron sputtering deposition is widely used to produce thin films and hard coatings because of its high deposition rate, ease of scaling, and the quality of the deposited films.<sup>1</sup> Among a variety of oxides, tin-doped indium oxide or Indium Tin Oxide (ITO) thin film is one of the most widely used material for microelectronic applications.<sup>2</sup> ITO conductive films have been used as transparent electrodes in optoelectronic devices such as liquid-crystal displays and solar cells.<sup>3</sup> The properties of ITO films have a strong relationship with their processing plasma characteristics.

Plasma diagnostics is widely being used to analyze plasma during the sputtering. Plasma is a gas ionized sufficiently so that the charge separation which can take place in it is small compared to its microscopic charge density. On a macroscopic scale, therefore, plasma is approximately neutral, although its principal constituents are charged ions and electrons. Information about fundamental plasma parameters, such as electron temperature, electron density, etc., are essential in order to evaluate the energy transport into the plasma. There are several diagnostic techniques employed for the determination of electron density and temperature which includes plasma spectroscopy,<sup>4</sup> Langmuir probe,<sup>5</sup> microwave and laser interferometries, and Thomson scattering.<sup>6–8</sup>

In this paper we report the studies on radio frequency (rf) plasma using Langmuir probe and optical-emission spectroscopy (OES). The plasma parameters such as ion density and electron temperature were determined and their dependence on properties of thin film deposited under similar plasma conditions were studied. Plasma parameters were determined for different rf powers keeping the distance from the target a constant.

### II. EXPERIMENTAL SETUP

The vacuum chamber used for the rf plasma analysis work was pumped down to a pressure of  $\sim 10^{-5}$  mbar by

means of a diffusion pump backed by rotary pump. An inert background gas (argon) was introduced into the chamber via a mass flow controller (MFC) up to a pressure of 0.01 mbar. The target used in the present study was a 2-in-diam ITO sintered disk containing 95 wt % of  $\text{In}_2\text{O}_3$  and 5 wt % of  $\text{SnO}_2$ .

Langmuir probe is one of the simplest techniques for obtaining information about the ions in plasma. A rf compensated Langmuir probe was used for plasma diagnostics (Fig. 1). The Langmuir probe assembly consists of a Tungsten wire, 0.5 mm in diameter and 5 mm in length, supported by a glass sleeve along with the rf compensating circuit. Probe current is measured for bias voltages in the range of  $-60$  to  $+60$  V. The probe voltage-current ( $V$ - $I$ ) characteristics are plotted for different rf powers (20–50 W). Great care was taken to prevent the probe feed wires being exposed to the plasma since this will contribute to the measured probe current. To ensure a clean probe surface, the probe wire was replaced frequently.

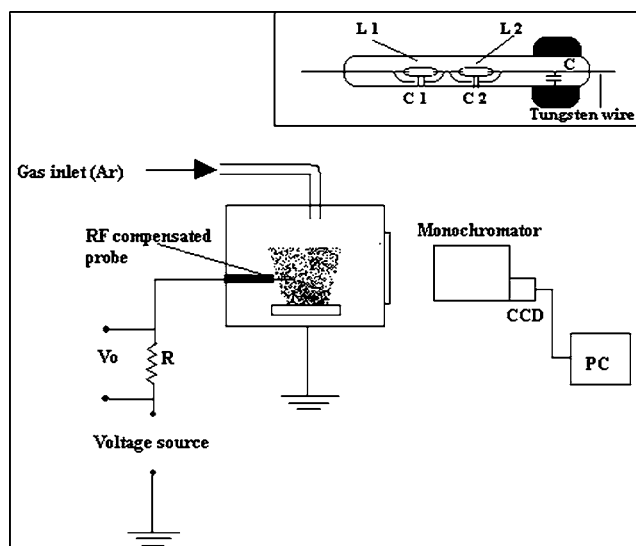


FIG. 1. Experimental setup for Langmuir probe and optical emission spectroscopic measurements.  $R$  is resistance across which the output voltage ( $V_0$ ) is measured. Inset shows the rf-compensated probe.  $L1$ , and  $L2$  are inductors, while  $C$ ,  $C1$ , and  $C2$  are capacitor.

<sup>a)</sup>Author to whom correspondence should be addressed; FAX: +91 484 2577595; electronic mail: mkj@cusat.ac.in

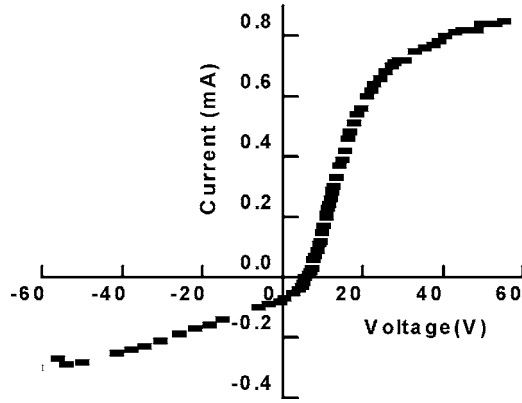


FIG. 2. Langmuir probe  $I$ - $V$  characteristics for a probe distance of 4 cm from the target and a rf power of 20 W.

To investigate the ionic species present in the rf plasma in detail OES of plasma plume generated by rf sputtering of ITO target was recorded using a 0.32 m monochromator and a charge-coupled device (CCD) detector. The OES were recorded through the side window of the chamber. The emission spectral data were collected from the plasma at a distance 4 cm from the target at various rf powers.

### III. RESULTS AND DISCUSSION

#### A. Langmuir probe studies

A typical Langmuir probe  $I$ - $V$  characteristics for a rf power of 20 W is shown in Fig. 2. The floating potential ( $V_f$ ) and plasma potential ( $V_p$ ) are determined from the Langmuir probe  $I$ - $V$  plot. The difference between plasma potential and floating potential ( $V_p - V_f$ ) gives a measure of energy of the sputtered particles bombarding the substrate.<sup>9</sup>  $V_p - V_f$  is plotted in Fig. 3 as a function of rf power. In the present investigation  $V_p - V_f$  shows a slight decrease with increasing rf power.

The ion saturation portion of the characteristics is used to determine the ion density.<sup>10</sup> The ion current drawn by the probe is given by the equation

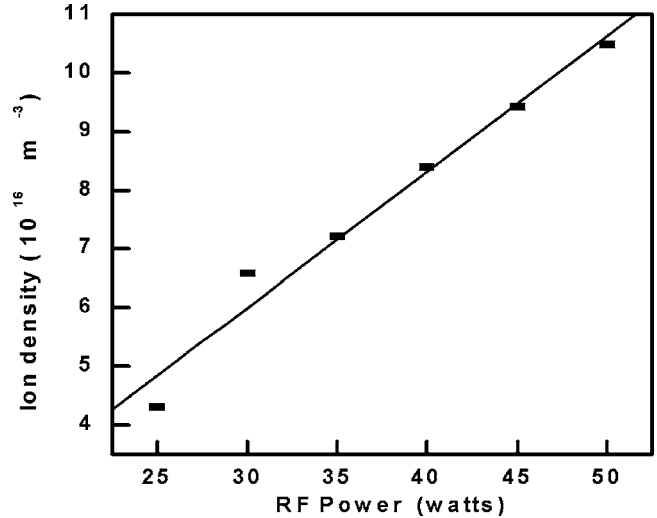


FIG. 4. Variation of ion density as a function of rf power.

$$I_i = \frac{Ae^{3/2}N}{2\sqrt{\pi}} \left( \frac{3T_e}{m_i} \right)^{1/2} \left( 1 - \frac{V - V_p}{T_e} \right)^{1/2}, \tag{1}$$

where  $A$  is the surface area of the probe,  $N$  is the plasma density,  $m_i$  is the ion mass, and  $T_e$  is the electron temperature in eV. Taking the derivative of  $I_i^2$  with respect to  $V$  and rearranging we get

$$N_i^2 = - \frac{4\pi m_i}{3A^2 e^3} \left( \frac{\partial I_i^2}{\partial V} \right). \tag{2}$$

The electron temperature is determined from the slope of the  $\ln(I)$ - $V$  curve of the probe in the region between  $V_f$  and  $V_p$  by the equation<sup>10</sup>

$$T_e = \frac{\partial V}{\partial \ln(I)}, \tag{3}$$

where  $I$  is the electron current.

Figures 4 and 5 show the dependence of ion density and electron temperature on rf power. Ion density is found to

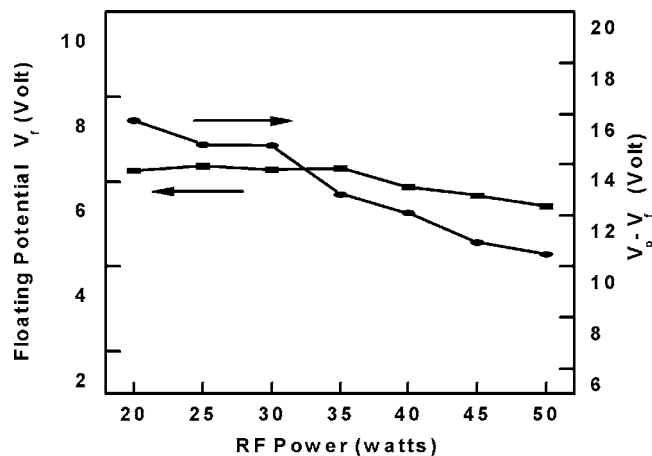


FIG. 3. Variation of floating potential ( $V_f$ ) and  $V_p - V_f$  with rf power.

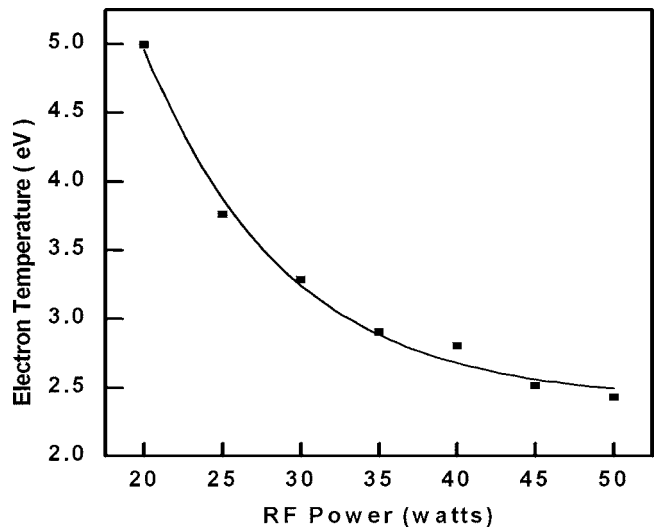


FIG. 5. Variation of electron temperature as a function of rf power.

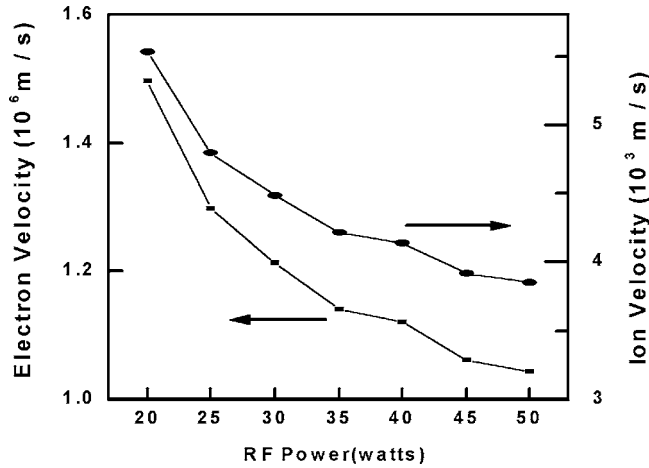


FIG. 6. Variation of electron velocity and ion velocity with rf power.

increase linearly with increase in rf power whereas electron temperature decreases with rf power. The increase in ion density is due to the greater ionization resulting from collisions that may occur at higher rf power. The drop in electron temperature and  $V_p - V_f$  is due to the increase in ion density.<sup>11</sup> The ion velocity and electron velocity were calculated using the following equations:<sup>12</sup>

$$v_e = \left( \frac{8kT_e}{\pi m_e} \right)^{1/2}, \quad (4)$$

$$v_i = \left( \frac{8kT_e}{\pi m_i} \right)^{1/2}, \quad (5)$$

where  $k$  is the Boltzmann constant,  $T_e$  is the electron temperature,  $m_e$  is the electron mass, and  $m_i$  is the ion mass. Variation of ion and electron velocities is shown in Fig. 6. Velocity of electrons is found to be of the order of  $10^6$  m s<sup>-1</sup> while that of ions is of the order of  $10^3$  m s<sup>-1</sup>.

## B. Optical emission studies

The rf plasma generated during the sputtering of ITO target was analyzed by recording the optical emission spectra to identify the ionic species in the plume. The spectral analysis revealed that the ionic species is mainly composed of argon ions. The identified species essentially comprises argon neutrals (Ar I), singly ionized argon (Ar II), doubly ionized argon (Ar III), indium neutral (In I), oxygen neutral (O I), and tin neutral (Sn I).<sup>13</sup> Figure 7 gives a typical optical emission spectrum taken at a rf power of 20 W. The spectral data are collected from the plasma at a distance of 4 cm from the target.

The optical emission spectral shows that the intensity of emission lines increases with increase of rf power. The variation of integral intensity of argon (I) at a wavelength of 811.5 nm with rf power is given in the inset of Fig. 7. The integral intensity is found to increase linearly with rf power. Increase of rf power causes more ionization, which in turn increases the population of various energy levels associated with the ions leading to the increase in integral intensity.

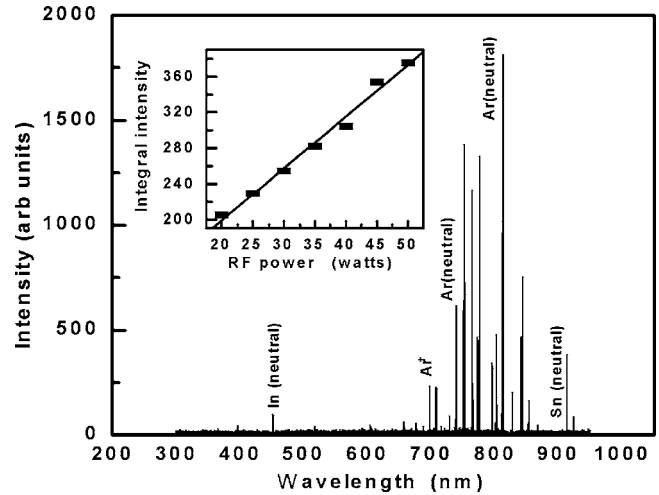


FIG. 7. Optical Emission Spectrum of rf plasma generated with ITO target at a rf power of 20 W and at a distance of 4 cm from the target. Inset shows the Variation of integral intensity of Argon (I) at a wavelength of 811.5 nm with rf power.

In order to correlate the plasma parameters with the observed film properties, Indium tin oxide thin films were deposited by rf magnetron sputtering at room temperature at a target to substrate separation of 4 cm by varying rf power. The films deposited at lower rf powers were polycrystalline and do not show any preferred orientation as seen from the x-ray-diffraction pattern (Fig. 8). These films show (222) and (440) diffraction peaks of indium oxide ( $\text{In}_2\text{O}_3$ ).<sup>14</sup> With increase in rf power, the intensity of these peaks reduced and the films oriented in the [100] direction, which was inferred from the appearance of (400) diffraction peak in the x-ray-diffraction pattern. The increase in ion density with rf power enhances the deposition rate, which leads to an increase in film thickness. The change in orientation of the grains may be due to this increase in thickness of the film.<sup>15</sup>

The film deposited at a rf power of 50 W was highly conducting also. The conductivity increased from 6 to 170 S/cm when the rf power was increased from 20 to 50 W. The increase in mobility of the carriers and

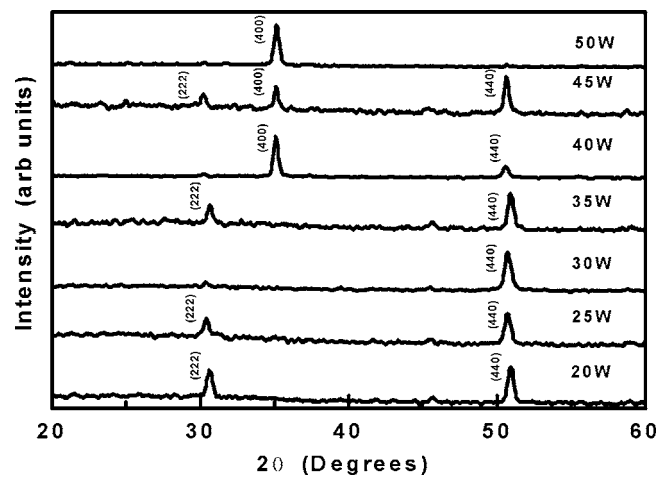


FIG. 8. X-ray-diffraction pattern of ITO thin films deposited at various rf powers for a target to substrate spacing of 4 cm.

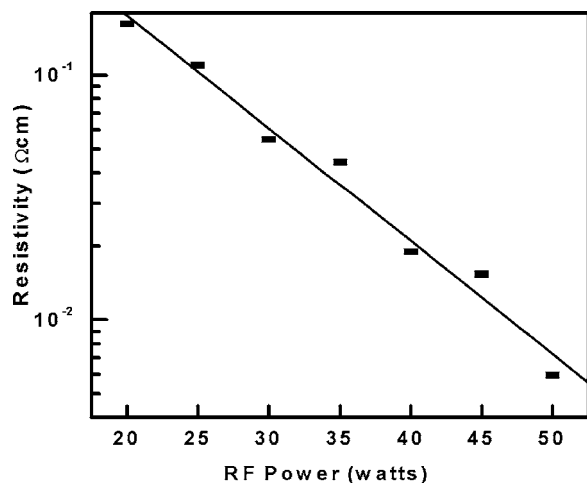


FIG. 9. Variation of resistivity of ITO thin films with rf power.

number of free carriers with increase in rf power increases the conductivity of the films.<sup>16</sup> Figure 9 shows the variation of resistivity of ITO thin films with rf power. The plasma studies showed that the ion density is high and the electron temperature is minimum at a rf power of 50 W, which resulted in best film properties at that particular power. The electron temperature and ion velocity attain a constant value at about 40 W. The rate of film deposition also more or less independent of the rf power above 40 W (Fig. 10).

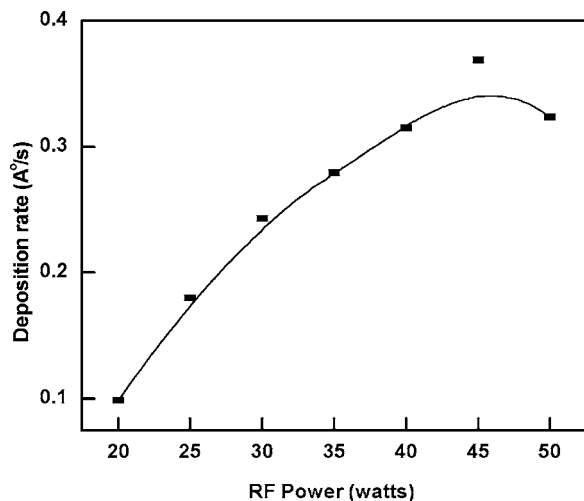


FIG. 10. Variation of film deposition rate with rf power.

#### IV. CONCLUSION

Langmuir probe and Optical Emission Spectroscopic (OES) studies were done to determine the plasma parameters. Different ionic species in the plasma were identified from the spectrum. The plasma parameters such as electron temperature, electron velocity, ion velocity, and ion density were determined by the Langmuir probe for various rf power. The Langmuir probe and OES studies were carried out for scaling the ion density with rf power. The observed plasma parameters were correlated with the thin films deposited under similar plasma conditions. The ion density and electron temperature were the highest for a rf power of 50 W and the best film properties were obtained at that particular rf power.

#### ACKNOWLEDGMENTS

This work was supported by Department of Science and Technology, Government of India. One of the authors (M.K.J.) wishes to thank Kerala State Council for Science, Technology and Environment for the financial assistance under SARD programme. Another author (N.M.) thanks Council of Scientific and Industrial Research for Junior research fellowship.

- <sup>1</sup>J. A. Thornton, *J. Vac. Sci. Technol.* **15**, 171 (1978).
- <sup>2</sup>I. Hamberg and C. G. Granqvist, *J. Appl. Phys.* **60**, R123 (1986).
- <sup>3</sup>P. K. Song, Y. Shigesato, M. Kamei, and I. Yasui, *Jpn. J. Appl. Phys., Part 1* **38**, 2921 (1999).
- <sup>4</sup>H. R. Griem, *Plasma Spectroscopy* (McGraw-Hill, New York, 1964).
- <sup>5</sup>R. H. Huddleston and S. L. Leonard, *Plasma Diagnostic Techniques* (Academic, London, 1965).
- <sup>6</sup>M. A. Heald and C. B. Wharton, *Plasma Diagnostic with Microwaves* (Wiley, New York, 1965).
- <sup>7</sup>M. C. M. Van de Sanden, J. M. de Regt, G. M. Janssen, J. A. M. Van der Mullen, D. C. Schram, and B. Van der Sijde, *Rev. Sci. Instrum.* **63**, 3369 (1992).
- <sup>8</sup>S. B. Cameron, M. D. Tracy, and J. P. Camaco, *IEEE Trans. Plasma Sci.* **24**, 45 (1996).
- <sup>9</sup>J. T. Gudmundsson, J. Alami, and U. Helmesson, *Appl. Phys. Lett.* **78**, 3427 (2001).
- <sup>10</sup>J. E. Heidenreich III, J. R. Paraszczak, M. Moisan, and G. Suave, *J. Vac. Sci. Technol. B* **5**, 347 (1987).
- <sup>11</sup>K. Deenamma Vargheese and G. Mohan Rao, *Rev. Sci. Instrum.* **71**, 467 (2000).
- <sup>12</sup>J. M. Hendron, C. M. O. Mahony, T. Morrow, and W. G. Graham, *J. Appl. Phys.* **81**, 2131 (1997).
- <sup>13</sup>J. R. Fuhr and W. L. Wiese, in *Handbook of Chemistry and Physics*, 79th ed., edited by D. R. Lide (CRC, Boca Raton, FL, 1998), pp. 10–53 and 10–80.
- <sup>14</sup>Joint Committee on Powder Diffraction Standards, Powder Diffraction File Card No. 6-416 (ASTM, Philadelphia, PA, 1967).
- <sup>15</sup>Y. S. Jung and S. S. Lee, *J. Cryst. Growth* **259**, 343 (2003).
- <sup>16</sup>C. G. Granqvist and A. Hultaker, *Thin Solid Films* **411**, 1 (2002).